[AMERICAN JOURNAL OF SCIENCE, VOL. 276, OCTOBER, 1976, P. 997-1022]

A PRELIMINARY INVESTIGATION OF STRONTIANITE DISSOLUTION KINETICS

JOHN L. SONDEREGGER,* KAY R. BROWER, and VERNON G. LeFEBRE

New Mexico Institute of Mining and Technology
Socorro, New Mexico 87801

ABSTRACT. A preliminary investigation of strontianite dissolution kinetics in aqueous solutions indicates that dissolution rates are controlled by reactions at the mineral surface. Dissolution rates were not affected by changes in stirring rates; the activation energy calculated for strontianite is 10 ± 2 kcal.

At pH values less than 4.0, the dissolution rate for strontianite is a linear function of a_{H^+}; the dissolution reaction is interpreted to be first order with respect to a_{H^+} and to result from H^+ diffusion or from the protonation of the CO_3^{2-} lattice anion and desorption as HCO_3^-. Experiments with different partial pressures of CO_2 indicate that H_2CO_3 has a catalytic effectiveness approximately 1 percent of that of the hydrogen ion. The effect of P_{CO_2} is interpreted to be dependent upon surface adsorption and is expressed using the Langmuir adsorption isotherm.

Forward reaction rates determined far from equilibrium are used to calculate back reaction rates. These data are consistent with a controlling mechanism that is first order with respect to Sr^{2+} or HCO_3^-. The rate-limiting step for the back reaction is interpreted to be the adsorption or deprotonation of HCO_3^-.

INTRODUCTION

Many investigators are now involved with describing quantitatively the kinetic parameters that affect mineral dissolution and precipitation, but recent work on carbonate precipitation and dissolution (Gaines and Heffner, 1973; Mitterer and Carter, 1973; Walls, 1973; Berner and Morse, 1974; Plummer and Mackenzie, 1974) has been largely restricted to studies of calcium and magnesium carbonates.

Strontianite is not a common sedimentary mineral, but its occurrence or a solid solution series in carbonate rocks may control the strontium concentration of ground waters in Missouri (Carpenter and Miller, 1969). This preliminary investigation was undertaken to determine the dissolution kinetics of this mineral, so that it might be included in models relating to the change of ground-water composition with time. Constant and variable volume batch reactors were used to study thermodynamically open systems subjected to a constant gas flow. Dissolution was studied at temperatures of 30°, 40°, and 50°C in order to determine that activation energy. Strontianite dissolution was investigated at varying conditions of pH and partial pressure of carbon dioxide to determine their effect upon dissolution. The experimental rate data provide information about activation energies, the extent of acid catalysis, mineral solubility products, and the rate-limiting step.

CARBONATE DISSOLUTION KINETICS

The dissolution of calcite has received more attention than that of any other carbonate mineral. A brief summary of recent approaches used

* Present address: Montana Bureau of Mines and Geology, Butte, Montana 59701

and models proposed for calcite dissolution provides a basic framework with which the dissolution of strontianite may be compared.

A synthesis of the existing calcite dissolution data was proposed by Curl (1968) in which he noted that three different rate-limiting mechanisms — reactant diffusion, product diffusion, and a surface chemical reaction — have been proposed to explain calcite dissolution behavior. His interpretation of mechanisms was restricted to diffusion control, and he suggested that at very low fluid velocities diffusion of product species limits dissolution, whereas at high fluid velocities the dissolution rate is limited by diffusion of the reactant species, H_2CO_3, to the mineral surface.

Berner and Morse (1974) determined calcite dissolution rates in pseudo-seawater to provide base rates for the study of dissolved species that inhibit calcite dissolution (see, also, Morse, 1974b). In their dissolution experiments, a constant pH was maintained by titrating acid (HCl) into the reaction vessel (Morse, 1974a), and the reaction rate was calculated from the rate of acid addition. They suggested that four different kinetic regimes exist when the calculated dissolution rate was plotted as a function of ΔpH, the equilibrium pH minus the experimental pH, as shown in figure 1 (Berner and Morse, 1974; also see Berner and Wilde, 1972). Because the initial calcium concentration of their solutions was that normally found in seawater, the total calcium concentration changed very little during their experiments (Berner and Morse, 1974), and the interpretation of the experimental data was necessarily restricted to the roles of H^+, H_2CO_3, HCO_3^-, and CO_3^{2-} upon calcite dissolution. Berner and Morse (1974) concluded that: (1) at pH values of 4.0 or less, calcite dissolution is diffusion controlled and independent of P_{CO_2}; (2) at pH values greater than 4.0, but for which ΔpH is greater than some critical

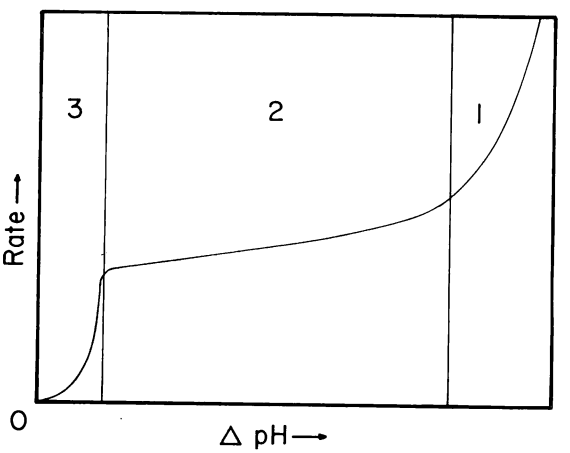

Fig. 1. Schematic plot of the rate of calcite dissolution as a function of ΔpH (after Berner and Morse, 1974).

value, which varied from 0.10 to 0.25, the dissolution rate is a linear function of ΔpH and shows a P_{CO_2} dependency; however, the dissolution rate as a function of pH is independent of P_{CO_2} for $P_{CO_2} \geq 10^{-2.0}$ (Berner and Morse, 1974, fig. 9); (3) at pH values greater than 4.0 and such that ΔpH is less than the critical value, the dissolution rate decreases sharply and then approaches equilibrium asymptotically. They interpret the first stage (pH $\leq$ 4.0) to represent a P_{CO_2}-independent, diffusion-controlled, rate-limiting condition, controlled by the flux of H^+ to the mineral surface or Ca^{2+}, HCO_3^-, and CO_3^{2-} away from the mineral surface. They interpret the second and third stages to be controlled by a surface process or processes.

EXPERIMENTAL PROCEDURES

Sample Preparation

A sample of strontianite from the Westphalia mining district, Germany, was obtained from Ward's Natural Science Establishment. The sample was reportedly from a vein deposit and was processed in the following manner:

1. All gangue minerals and a portion of the outside of the vein were removed, the sample was broken into approximately half-inch pieces and crushed in a tool-steel piston-style sample crusher.
2. The sample was spread on white paper, and the impurities, mainly galena, sphalerite, and iron hydroxide coatings, were removed by hand.
3. The sample was dry sieved using brass 30-mesh and nylon 100- and 200-mesh screens, the <30 but >100 mesh fraction was visually reexamined to remove impurities using a high-intensity lamp and a biology pick.
4. The <30 but >100 mesh material from step (3) was washed first with 0.1 N reagent-grade hydrochloric acid and then with four rinses of distilled water and a final rinse on the 100-mesh screen, followed by drying in a vacuum. The samples were then divided, using a small vibrating sample splitter, and sealed in glassine paper packets for storage prior to use. The mean sample weight was 18.716 g with a standard deviation of 0.208 g.

Strontianite Composition

The strontianite purity was initially confirmed by X-ray diffraction, using fluorite as an internal standard. The pattern showed no detectable evidence of a solid solution substitution for Sr in the mineral lattice. This was confirmed by the chemical analysis shown in table 1.

TABLE 1

Analysis of strontianite for impurities, in parts per million

Element	Ca	Mg	Ba	Na	K	Li
ppm	2600	3.8	850	4.1	<1	<1

Element	Fe	Mn	Pb	Zn	S	Cl	P
ppm	23	<1	<1	<1	<10	<20	<25

Reaction Vessel Design

A cylindrical reaction vessel was constructed from lucite with a permanently attached base and a removable top. The inside diameter and height are 11.3 and 15.3 cm, respectively; a liter of water occupies about two thirds of the available volume. The sample was added to the aqueous phase through a glass funnel inserted through a hole in the top of the reaction vessel. The vessel was placed upon a variable-speed magnetic stirring unit, and a fixed rate of stirring was provided by an ovoid Teflon-coated magnetic spin bar; the ovoid shape was selected to minimize grinding of the sample. The stirring rate used did not maintain the +100-mesh strontianite in suspension; the sample was distributed on the bottom of the vessel outward from the center where the spin bar was positioned.

Commercially prepared nitrogen and carbon dioxide gases with impurities less than 1 percent were used in this study. The gas or gas mixture was introduced into the aqueous phase through a vertical glass tube, which has a sintered glass plug at the bottom. Such gas-dispersion tubes aid greatly in saturating rapidly the fluid phase with the gas phase, because an increased interphase contact area results from the large number of small gas bubbles produced by passage of the gas through the sintered glass. The gases were passed into a 1-liter Erlenmeyer flask containing 900 ml of water at ambient temperature (28.5 ± 1.0°C) for presaturation of the gas with water vapor prior to introduction into the reaction vessel. There was no measurable loss of water.

The heat source for the experiments consisted of a 100-watt standard frosted glass light bulb for 30°C and a 150-watt infrared bulb for 40° to 50°C. A thermistor probe extended into the aqueous phase from the top of the reaction vessel and was calibrated with an alcohol thermometer having 0.2° divisions, which was inserted in the same manner. Temperature variation of the aqueous phase was less than 0.5°C.

The reaction progress was monitored manually by acid titration for dissolution at fixed pH and by pH change for "free drift" dissolution. The pH was measured with a Beckman model 39013 combination electrode and a Corning model 12 pH meter. Buffers with pH values of 4.015 and 6.995 at 30°C were used to calibrate the pH meter and electrode. Instrumental drift during an experiment generally was less than ±0.02 pH units as determined using buffer solutions before and after an experimental run; however, a confidence limit of ±0.05 pH units is used to compensate for any additional errors that might have existed during the experiments.

Data Treatment

The pH values as a function of time for free drift experiments were recorded manually by the experimenter. The data required curve fitting to provide pH values for times between measurements. Also, curve fitting of the data prior to analysis reduces the effect of random instrumental

or observer error and is a standard practice prior to differential analysis of rate data (Levenspiel, 1972, p. 67-69). The curve fitting was accomplished by hand with a flexible curve to prevent bias of the data in the direction of a kinetic model paralleling the mathematical expression of the curve-fitting equation.

In experimental systems the gas phase being bubbled through the reaction vessel must be saturated with the solvent to prevent loss of the solvent to the gas phase. At pressures of 1 atm or less the fugacity coefficients of most gases are very close to unity, and the fugacity of the i^{th} gas, f_i, may be expressed by the ideal gas law

$$f_i = N_i P_{tot} = P_i \tag{1}$$

where N_i is the mole fraction of the i^{th} gas in the gas mixture, P_{tot} is the total pressure, and P_i is the partial pressure of the i^{th} gas (Denbigh, 1966). When considering a system with a fixed overpressure, an aqueous phase, and one or more gases being bubbled through the aqueous phase, the partial pressure of the i^{th} gas being bubbled through the reaction vessel may be expressed as

$$P_i = N_i(P_{tot} - P_{H_2O}) \tag{2}$$

where P_i is the partial pressure of i^{th} gas, N_i is the mole fraction of the i^{th} gas (excluding H_2O), and P_{H_2O} is the vapor pressure of water at the temperature of interest. Equations (1) and (2) were used in calculating the partial pressure of carbon dioxide in this study.

The vapor pressures of water at 30°, 40°, and 50°C are 0.0419, 0.0728, and 0.135 atm, respectively. The experiments were conducted in Socorro, N.M., where the average barometric pressure is approximately 650 mm of mercury or 0.855 atm. With a total pressure of 0.855 atm, the calculated carbon dioxide partial pressures when $N_{CO_2} = 1.0$ at 30°, 40°, and 50°C are 0.813, 0.782, and 0.720 atm respectively.

The activities and molalities of all species in solution were calculated by the method outlined by Garrels and Christ (1965, p. 76-83) with the aid of a computer program, CATCALC, written for the dissolution of carbonate minerals under a fixed partial pressure of carbon dioxide. The measured variable, pH, and the constraint of electrical neutrality permit an iterative solution of a series of simultaneous equations despite the fact that carbon dioxide is not conserved in the system of interest.

The equations necessary for these calculations (ignoring ion pairs) are:

$$K_w = a_{H^+}\, a_{OH^-} \tag{3}$$

$$K_O = a_{H_2CO_3}/P_{CO_2} \tag{4}$$

$$K_1 = (a_{H^+}\, a_{HCO_3^-})/a_{H_2CO_3} \tag{5}$$

$$K_2 = (a_{H^+}\, a_{CO_3^{2-}})/a_{HCO_3^-} \tag{6}$$

and

$$(m_{H^+}) + 2(m_{Sr^{2+}}) = (m_{HCO_3^-}) + 2(m_{CO_3^{2-}}) + (m_{OH^-}) \tag{7}$$

This results in a system of five equations and seven variables, of which the two independent variables, pH and P_{CO_2}, are known.

The only assumptions employed in the calculations are that equilibrium is maintained by all gaseous and aqueous species, that activities of unity are assigned to the solid phase and water, that ion pairs are insignificant (Jacobson and Langmuir, 1974), and that the activity coefficients are correct. The second assumption has been shown to contribute negligible error (Helgeson, 1967). The assumption of equilibrium between gaseous and aqueous species implies that the experimental conditions fall in Curl's (1968) low-velocity [of fluid flow] region. For the reaction

$$CO_{2(aq)} + H_2O \rightarrow H_2CO_3 \tag{8}$$

the reaction rate may be expressed

$$-d(CO_{2(aq)})/dt = k(CO_{2(aq)}),\ k = 0.03\ sec^{-1} \tag{9}$$

where $CO_{2(aq)}$ is dissolved carbon dioxide (Kern, 1960). Considering that the experiments range in length from 1 to 7 hrs, the assumption that the bulk solution is in equilibrium with respect to dissolved and gaseous species seems reasonable. The sequence of steps employed in the calculation are described by Garrels and Christ (1965, p. 76-81). The values of the constants used are listed in table 2.

The systems investigated were maintained at various fixed partial pressures of carbon dioxide. Consequently, the concentrations of carbonate species depended upon contributions to or withdrawals from the gas phase as well as the quantity resulting from carbonate mineral dissolution. Similarly, the pH was affected by the carbon dioxide partial pressure (compare Garrels and Christ, 1965, chap. 3, cases 1 and 4) or externally controlled by acid titration. The only constituent that was con-

TABLE 2
Constants used in program CATCALC

Reaction	pK at 30°C	pK at 40°C	pK at 50°C	Reference
$H_2O = H^+ + OH^-$	13.883	13.535	13.262	*
$H_2O + CO_{2(g)} = H_2CO_3$	1.53	1.64	1.70	*
$H_2CO_3 = H^+ + HCO_3^-$	6.33	6.30	6.29	*
$HCO_3^- = H^+ + CO_3^{2-}$	10.29	10.22	10.17	*
$SrCO_{3(s)} = Sr^{2+} + CO_3^{2-}$	9.27	9.33	9.40	**
Constants used in the equation $-\log \gamma_i = \frac{Az_i^2 \sqrt{I}}{1 + \mathring{a}_i B \sqrt{I}} + 0.1\, z_i\, I$	T = 30°C	T = 40°C	T = 50°C	
A	0.5144	0.5244	0.5354	***
B ($\times 10^{-8}$)	0.3292	0.3310	0.3329	***

* Garrells and Christ, 1965.
** Estimated from affinity plots.
*** Helgeson, 1967.

served in the aqueous phase was strontium. The reaction rate, as used in this study, is defined as

$$R = dm_{Sr^{2+}}/dt \tag{10}$$

for constant reactor volumes and was determined from the finite derivates $\Delta m_{Sr^{2+}}/\Delta t$ calculated from the curve-fitted pH values for the free drift experiments.

Sources of Error

Several sources of error existed under the experimental conditions. Visual analysis of the sample material from both before and after experimental runs showed a considerable amount of finer material that was not removed by seiving. There was no noticeable change in the amount of the fines, but their presence prevented visual determination of surface area and evaluation of possible grinding of the sample by the magnetic stirrer. The sample material was dispersed outward from the center of stirring, and it was not noted that it was drawn back to the pivot point. Although some grinding of the sample material undoubtedly occurred, the amount is not believed to be significant.

A second source of error, which might have been adequately controlled, was that of the shearing potential developed at the electrode-solution interface. The partial pressure of carbon dioxide was checked by pH measurement. Agreement between calculated and observed pH values to within ±0.02 pH units could be achieved only when the system was unstirred (almost all fluid motion resulting from the bubbling of gas through the reaction vessel). When the solution was stirred, the pH was always found to be less than for unstirred conditions. This effect was most pronounced at low pH values and high partial pressures of carbon dioxide; the maximum variance recorded was 0.115 pH unit at 30°C. It was found to vary also with temperature, ionic strength, stirring rate, and the composition of the solution; the shape of the reaction vessel and the electrode design are additional factors that probably should be considered. The time restrictions placed upon the experimental work did not permit the determination of calibration curves for all the necessary variables under the experimental conditions. Consequently, the observed pH values are thought to be accurate only to within ±0.05 pH units for pH values greater than 4.4.

EXPERIMENTAL RESULTS

Introduction

The experimental data for dissolution of strontianite may be divided into three subgroups:

1. The effect of pH on strontianite dissolution determined by acid titration at 40°C with continuous removal of carbon dioxide by a stream of nitrogen.
2. The effect of various partial pressures of carbon dioxide on strontianite dissolution determined by acid titration at 40°C and pH = 4.5.

3. The dissolution of strontianite at 30°, 40°, and 50°C with a fixed carbon dioxide partial pressure, determined by free drift monitoring of pH.

By holding all variables except pH or P_{CO_2} constant, the effect of pH and P_{CO_2} upon strontianite dissolution can be determined. The results of this study include the determination of activation energy and solubility product for strontianite dissolution and an interpretation of the mechanism that limits its dissolution rate.

Titration Experiments

The effect of pH.—The rate of strontianite dissolution was investigated under a nitrogen atmosphere at 40°C for pH values of 1.5, 2.5, 3.5, 4.5, 5.5, and 6.5. In order to maintain greatly undersaturated conditions for each of the experiments, nitrogen gas was bubbled through the system to remove, as CO_2, the carbonic acid resulting from strontianite dissolution. Each experiment was run for 1 hr, and the acid consumption for the period from 20 to 40 min was used to calculate the rate of acid addition at the experimental pH. Acid consumption during the initial and final stages was within 10 percent of the 20- to 40-min consumption. The reaction rate was determined by the number of moles of HCl added per min to maintain the predetermined pH. The reaction rate varied over three orders of magnitude, while the hydrogen ion activity varied over five orders of magnitude.

To compare these results with the results of the temperature-dependent strontianite dissolution, the reaction rate must be expressed in terms of $(dm_{Sr^{2+}}/dt)$. These strontianite dissolution reactions were conducted by titrating hydrochloric acid into the system to maintain the desired pH, and carbon dioxide was removed by the stream of nitrogen gas. Therefore, the reaction may be written as

$$SrCO_3 + 2H^+ + 2Cl^- = Sr^{2+} + 2Cl^- + CO_{2(g)} + H_2O \quad (11)$$

and the reaction rate, R, is

$$R = (dm_{Sr^{2+}}/dt) + (m_{Sr^{2+}}/M_{H_2O})\,(dM_{H_2O}/dt) = \tfrac{1}{2}\,[(dm_{H^+}/dt) + (m_{H^+}/M_{H_2O})\,(dM_{H_2O}/dt)] \quad (12)$$

where M_{H_2O} is the mass of water. The second term is a volume correction, required to compensate for dilution effect of the added acid. Figure 2 is a plot of the calculated log R versus pH for strontianite dissolution at 40°C under a continuously renewed N_2 atmosphere. The data suggest that two separate controls upon the dissolution rate exist. Under low pH conditions, the dissolution rate seems to be controlled by a process that is approximately first order with respect to hydrogen ion activity, because the slope of a line connecting the first three data points is nearly minus one (−0.92). At higher pH conditions, pH greater than approximately 4.0, some other condition becomes the rate-limiting factor. This second stage does not seem to be entirely independent of pH but has a small

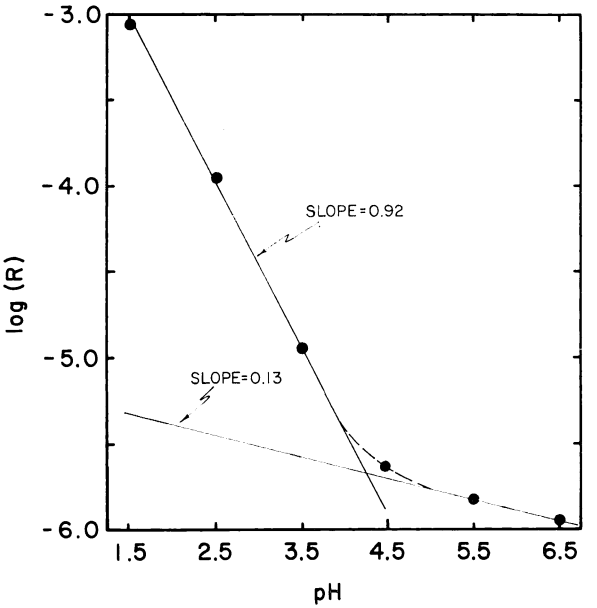

Fig. 2. Plot of the logarithm of the reaction rate (moles•min^{-1}) versus pH for strontianite dissolution at 40°C, P_{N_2} = 0.782 atm, and P_{H_2O} = 0.073 atm. The reaction rate was calculated using equation (12). The slope in the low pH region is —0.92, which is believed to represent a first-order rate-limiting step dependent upon a_{H^+}. Carbonate species were removed by a continuous stream of N_2 gas.

empirical exponential coefficient, which can be shown by the slope of a line connecting the data points at pH's of 5.5 and 6.5. The data may be represented by an equation of the form

$$R = k_1(a_{H^+})^{0.92} + k_2(a_{H^+})^{0.13} \tag{13}$$

where $k_1 = 2.05 \times 10^{-2}$, $k_2 = 8.65 \times 10^{-6}$, where R, k_1, and k_2, are expressed in moles per min, and the exponents come from the slopes of straight lines fitted to the data in figure 2.

The nature of this second term in equation (13) has not been determined, but two regions characterized by different rate-limiting mechanisms have been shown to exist. The strontianite dissolution rate is, within experimental error, a first-order function of hydrogen ion activity at pH values less than 4.0, which suggests diffusion control by H^+ to the mineral surface or by Sr^{2+}, H_2CO_3, or possibly HCO_3^- into the bulk solution. At higher pH values another mechanism, possibly either a reaction involving water at the mineral surface or the effect of a small but increasing amount of H_2CO_3 and HCO_3^-, controls the reaction rate. Because this aspect of the experimental work was conducted under a continuously renewed nitrogen atmosphere, carbon dioxide resulting from mineral dissolution was almost completely removed from the system. The effect

of carbonate species in solution is believed minimal, for reasons discussed in the next section.

Effect of P_{CO_2}

The effect of carbon dioxide partial pressure upon strontianite dissolution was investigated by streaming mixtures of carbon dioxide and nitrogen gases at 40°C. The P_{CO_2} conditions studied were 0.0, 0.20, 0.39, and 0.78 atm. To provide identical starting pH values, each experimental run had an initial pH of 4.02, which required acid addition for the P_{CO_2} values of 0.0, 0.20, and 0.39 atm. The pH was maintained at 4.5 by titrating 0.094 normal hydrochloric acid into the reaction vessel. The amount of acid added during the time period from 20 to 40 min after the start of the experiment was used to calculate the rate of acid addition. At a pH of 4.5, H_2CO_3 is the dominant hydrated carbonate species in solution, and the dissolution reaction may be written as

$$SrCO_3 + 2\ H^+ = Sr^{2+} + H_2CO_3 \qquad (14)$$

for the experimental conditions. Once the pH of 4.5 has been established, the reaction rate may be expressed using equation (12).

Figure 3 is a plot P_{CO_2} versus the reaction rate calculated from equation (12). The partial pressure of carbon dioxide was calculated from equation (2) where N_i is the mole fraction of carbon dioxide in the CO_2–N_2 mixture. It can be seen from figure 3 that the relationship between the dissolution rate of strontianite and P_{CO_2} is definitely nonlinear.

In the next section of this paper, we investigate this nonlinear relation between P_{CO_2} and R to determine whether it is consistent with an adsorption isotherm for CO_2.

Many gas-phase reactions catalyzed by elementary reactions occurring at an interface, such as the walls of a reaction vessel, are found to have reaction rates that vary with the surface area of the vessel. Investigations of gas adsorption at solid surfaces has led to the recognition of several basic types of adsorption-pressure relationships. The mathematical relationship between the amount of gas adsorbed by the solid phase of interest and the gas pressure at constant temperature is called isotherm. In cases where chemisorption occurs at the interface, the Langmuir adsorption isotherm is generally the best equation for representing the experimental data (Maron and Prutton, 1958).

The Langmuir adsorption isotherm equation may be expressed as

$$\theta = bP/(1 + bP) \qquad (15)$$

where θ is the fraction of the experimental surface covered by adsorbed gas, b is an empirical constant, and P is the partial pressure of the gas (Maron and Prutton, 1958). The amount of gas adsorbed per unit area of absorbent, y, should be proportional to the fraction of the surface covered and may be represented as

$$y = k_1\theta = k_1bP/(1 + bP) = aP/(1 + bP) \qquad (16)$$

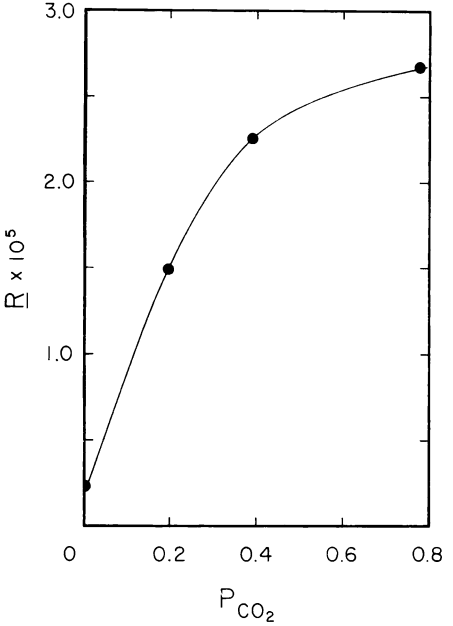

Fig. 3

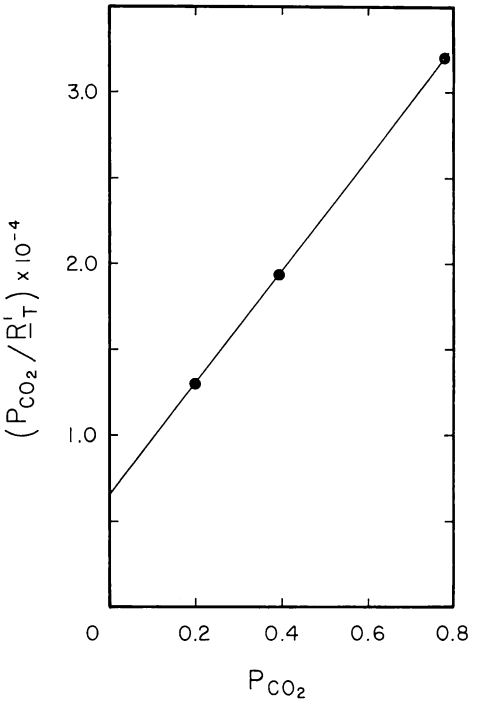

Fig. 4

Fig. 3. Plot of the dissolution rate of strontianite at 40°C and pH = 4.5 versus P_{CO_2}. The dissolution rate was calculated using equation (12).

Fig. 4. Plot of P_{CO_2}/R' versus P_{CO_2} for strontianite dissolution at 40°C and pH = 4.5. This plot demonstrates the applicability of the Langmuir adsorption isotherm as expressed by equation (17), assuming $y = R'$. The linearity of the data points demonstrates that R', the CO_2 contribution to the reaction rate, is proportional to θ, the fraction of the mineral surface covered by the adsorbed gas.

where k_1 is the proportionality constant, and $a = k_1 b$ (Maron and Prutton, 1958). Rearrangement of equation (16) yields:

$$P/y = (1/a) + (b/a)P \qquad (17)$$

If the reaction of interest is compatible with the Langmuir adsorption isotherm, a plot of P/y versus P should yield a straight line with slope of b/a and an intercept of 1/a.

If, under experimental conditions, variables such as total pressure, temperature, and pH are held constant, the change in the dissolution rate of the mineral in question may be related to the changing partial pressures of the gases in the gaseous phase. The assumption that the reaction rate is related to the fraction of the mineral surface that has adsorbed a carbonate species permits the application of the Langmuir adsorption isotherm to dissolution kinetics. This assumption, a simplified approximation of the actual processes occurring at the mineral surface,

allows an initial investigation of the role of dissolved gases on mineral dissolution kinetics. Such studies are of particular interest when the gas involved hydrates to form a weak (associated) acid, such as carbonic acid, which may catalyze the mineral dissolution reaction.

Application of the Langmuir adsorption isotherm to this study was accomplished by evaluating the change in reaction rate as a function of P_{CO_2}, assuming concurrent contributions to the reaction rate, using the relationship

$$R = f(a_{H^+}) + g(P_{CO_2}) + h \tag{18}$$

where, at the temperature of interest, R is observed reaction rate (mole• min^{-1}), f is a rate function describing the effect of hydrogen ion activity, g is a rate function describing the effect of carbon dioxide pressure, and h is a rate function of any additional unknown variables. If all known variables except the partial pressure of carbon dioxide are held constant and h is assumed to be negligible, the function g may be expressed as

$$g(P_{CO_2}) = (R - R_{P_{CO_2}=0}) = R' \tag{19}$$

where $R_{P_{CO_2}=0}$ is the experimental reaction rate determined by bubbling 100 percent nitrogen gas through the reaction vessel. Setting y in equation (17) equal to R' assumes that the increase in dissolution rate is related to an adsorption mechanism and provides a test of this assumption.

Figure 4 is a plot of P_{CO_2}/R' versus P_{CO_2}. The linearity of the points demonstrates that the kinetic effect of the partial pressure of carbon dioxide on strontianite dissolution is satisfactorily represented by the Langmuir adsorption isotherm. This strongly suggests, but does not prove conclusively, that the rate-limiting step for the forward (dissolution) reaction is related to an adsorption mechanism. The dissolution of strontianite with P_{CO_2} values of 0.0, 0.20, 0.39, and 0.78 atm was conducted at an artificially maintained pH of 4.5. For this reason, none of the reactions proceeded as far as 1 percent of completion. Consequently, the reaction rate is applicable only to conditions far from equilibrium where the back reaction should be insignificant (Gardiner, 1969).

Free Drift Experiments

Effect of temperature.—Strontianite dissolution was investigated at temperatures of 30°, 40°, and 50°C with carbon dioxide partial pressures of 0.81, 0.78, and 0.72 atm, respectively, to determine the activation energy of the dissolution reaction and to investigate the kinetics as the reaction proceeds toward equilibrium. The experimental system was left open to the atmosphere to provide a fixed overpressure on the system. Minor fluctuations in barometric pressure were not regarded as significant (Garrels, Thompson, and Siever, 1960) and were not monitored.

Investigations of strontianite solubility are not as numerous as those dealing with calcite. The values cited in the literature for the thermodynamic equilibrium constant (frequently referred to as the thermo-

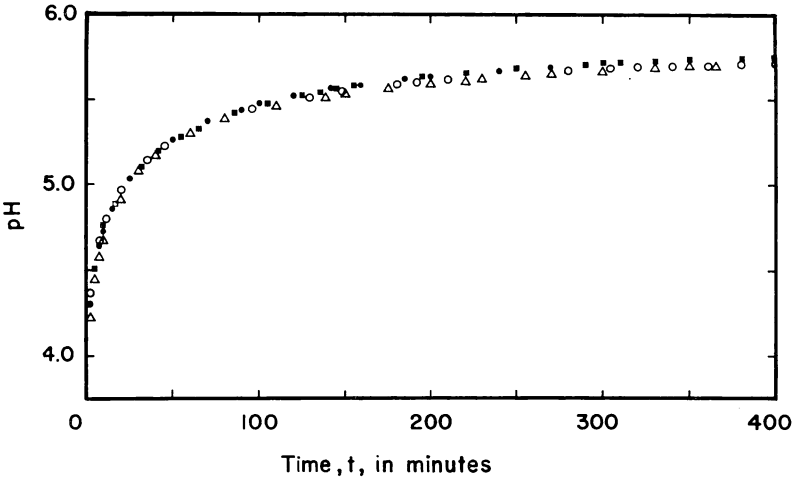

Fig. 5. Plot of experimental pH values for strontianite dissolution at 40°C and 0.78 atm P_{CO_2}. The four symbols represent the four runs conducted under these conditions; the open circle represents the unstirred experiment.

dynamic solubility product, K_{sp}) range over two orders of magnitude. Generally accepted values range from $10^{-9.15}$ to $10^{-9.6}$ at 25°C, but it seemed advisable to determine the thermodynamic solubility product from the experimental data. The molal solubility and solubility product values used for subsequent calculations were determined, using the affinity method of Prigogine, Outer, and Herbo (1948), to be: 3.82×10^{-3} moles of Sr^{2+} per Kg H_2O at 30°C ($pK_{sp} = 9.27, \pm 0.1$, equilibrium pH = 5.79 ± 0.05); 3.18×10^{-3} moles of Sr^{2+} per Kg H_2O at 40°C ($pK_{sp} = 9.33, \pm 0.1$, equilibrium pH = 5.81 ± 0.05); and 2.69×10^{-3} moles of Sr^{2+} per Kg H_2O at 50°C ($pK_{sp} = 9.40, \pm 0.1$, equilibrium pH = 5.82 ± 0.05). The pK_{sp} value at 25°C is calculated to be 9.235 ± 0.1, which is in excellent agreement with the values 9.22 and 9.25 calculated from the data of Garrels, Thompson, and Siever (1960) and from the National Bureau of Standards Technical Notes 270-3 and 270-5, respectively.

The reproducibility of the experimental data is demonstrated in figure 5, where four experimental runs at 40°C are plotted. Agreement during the first 200 min is excellent. From 200 to 400 min the divergence of experimental points is greater but well within the range of experimental error discussed earlier. Stirred and unstirred experiments proceeded at the same rate. Table 3 contains representative raw data for the three temperatures investigated.

The molalities of all aqueous species and the activities of all aqueous species other than H^+ were calculated using a computer program as discussed previously. Comparison of the calculated strontium concentrations with atomic absorption analyses of samples taken at the end of the experiment are in complete agreement within the analytical limits of the equipment (±10 percent) under routine conditions. The atomic absorption

TABLE 3

Raw data from free drift experiments

Temperature = 30°C, P_{CO_2} = 0.81 atm. Time in min since start of dissolution.

Time	pH	Time	pH	Time	pH	Time	pH	Time	pH
0	3.978					68	5.215	160	5.461
1	4.140	13	4.687	30	4.959	72	5.233	175	5.484
2	4.230	14	4.712	32	4.974	78	5.260	176	5.480
3	4.310	15	4.732	34	4.998	84	5.281	190	5.498
4	4.375	16	4.757	36	5.013	90	5.304	202	5.514
5	4.432	17	4.774	38	5.031	98	5.327	210	5.522
6	4.483	18	4.795	40	5.046	106	5.348	222	5.536
7	4.526	19	4.810	44	5.074	114	5.370	235	5.550
8	4.566	20	4.827	48	5.103	122	5.389	250	5.566
9	4.592	22	4.860	52	5.128	130	5.406	270	5.579
10	4.615	24	4.885	56	5.153	140	5.425	291	5.597
11	4.637	26	4.909	60	5.175	151	5.447	305	5.609
12	4.660	28	4.938	64	5.197			315	5.612

Temperature = 40°C, P_{CO_2} = 0.78 atm. Time in min since start of dissolution.

Time	pH	Time	pH	Time	pH	Time	pH	Time	pH
0	4.003					105	5.477	210	5.649
1	4.178	22	4.973	62	5.317	110	5.490	220	5.660
2	4.301	24	5.002	64	5.327	115	5.501	230	5.667
3	4.385	26	5.031	66	5.337	120	5.513	240	5.675
4	4.452	28	5.054	68	5.345	125	5.524	250	5.684
5	4.511	30	5.076	70	5.356	130	5.537	260	5.691
6	4.562	32	5.099	72	5.365	135	5.547	270	5.699
7	4.606	34	5.122	74	5.372	140	5.554	280	5.705
8	4.647	36	5.139	76	5.381	145	5.563	290	5.710
9	4.686	38	5.159	78	5.389	150	5.572	300	5.715
10	4.714	40	5.174	80	5.398	155	5.581	310	5.722
11	4.743	42	5.193	82	5.405	160	5.588	320	5.726
12	4.770	44	5.206	84	5.412	165	5.596	330	5.730
13	4.802	46	5.222	86	5.420	170	5.603	340	5.735
14	4.817	48	5.234	88	5.425	175	5.610	350	5.739
15	4.839	50	5.247	90	5.435	181	5.618	360	5.744
16	4.860	52	5.259	92	5.441	185	5.622	370	5.745
17	4.883	54	5.274	94	5.445	190	5.629	380	5.750
18	4.904	56	5.284	96	5.451	195	5.634	390	5.755
19	4.925	58	5.294	98	5.457	200	5.639	400	5.758
20	4.943	60	5.305	100	5.462			405	5.759

Temperature = 50°C, P_{CO_2} = 0.72 atm. Time in min since start of dissolution.

Time	pH	Time	pH	Time	pH	Time	pH	Time	pH
0	4.029					110	5.651	215	5.763
1	4.242	24	5.201	66	5.521	115	5.660	220	5.766
2	4.380	26	5.231	68	5.530	120	5.669	225	5.767
3	4.486	28	5.258	70	5.539	125	5.677	230	5.770
4	4.565	30	5.275	72	5.547	130	5.683	235	5.772
5	4.637	32	5.300	74	5.553	135	5.692	240	5.774
6	4.692	34	5.321	76	5.560	140	5.699	250	5.779
7	4.750	36	5.341	78	5.567	145	5.705	260	5.784
8	4.786	38	5.359	80	5.574	150	5.710	270	5.787
9	4.835	40	5.358	82	5.583	155	5.716	282	5.792
10	4.872	42	5.373	84	5.590	160	5.721	290	5.793
11	4.908	44	5.387	86	5.594	165	5.721	301	5.797
12	4.939	46	5.398	88	5.601	171	5.730	310	5.799
13	4.965	48	5.412	90	5.605	175	5.736	320	5.802
14	5.001	50	5.433	92	5.612	180	5.738	330	5.803
15	5.024	52	5.445	94	5.617	185	5.742	340	5.805
16	5.050	54	5.459	96	5.620	190	5.746	350	5.807
17	5.074	56	5.470	98	5.625	195	5.748	360	5.808
18	5.094	58	5.480	101	5.632	200	5.752	370	5.810
19	5.113	60	5.490	104	5.637	205	5.757	380	5.811
20	5.133	62	5.501	106	5.644	210	5.759	390	5.812
22	5.170	64	5.512	108	5.646			400	5.814

analyses are not consistently higher or lower than the values determined from the program; thus, systematic error in the program constants is probably minimal or compensating.

An empirical kinetic equation, frequently found applicable for the congruent dissolution of simple minerals (see Campbell and Nancollas, 1969; Liu and Nancollas, 1971) may be written for strontianite dissolution as

$$R = dm_{Sr^{2+}}/dt = k[(m_{HCO_3^-}{}_s) - (m_{HCO_3^-}{}_t)]^n \quad (20)$$

where R is the observed reaction rate, k is an empirical rate constant, $m_{HCO_3^-}{}_s$ is the molality of HCO_3^- in solution at saturation, $m_{HCO_3^-}{}_t$ is the molality of HCO_3^- at time t, and n is an empirical constant, assumed to be the order of the reaction. For cases where n = 1.0, equation (20) reduces to the Nernst equation, which is commonly used to describe diffusion-controlled reactions. The value of n may be determined by plotting log R versus log $[(m_{HCO_3^-}{}_s) - (m_{HCO_3^-}{}_t)]$. If the empirical value of n is approximately one, equation (20) may be rearranged and integrated to yield

$$\log [(m_{HCO_3^-}{}_s) - (m_{HCO_3^-}{}_t)] = kt + C \quad (21)$$

where t is the time since the experiment started and C is the integration constant. Plotting log $[(m_{HCO_3^-}{}_s) - (m_{HCO_3^-}{}_t)]$ against time yields a straight line for first-order reactions and the rate constant, k, is the slope of this straight line.

Figure 6 is a plot of log R versus log $[(m_{HOC_3^-}{}_s) - (m_{HCO_3^-}{}_t)]$ and shows that the experimental data for 50°C deviate excessively and systematically from the expected behavior, which suggests that more than one mechanism may be operative over the experimental range. The data for 40° and 50°C approximate a first-order reaction having an average value for n of 0.92. Consequently, equation (21) has been used to evaluate a possible first-order reaction mechanism. Figure 7, a plot of log $[(m_{HCO_3^-}{}_s) - (m_{HCO_3^-}{}_t)]$ versus time since the start of the experiment, provides a test of the first-order hypothesis. Because the experimental data plot in nearly straight lines, it is apparent that the experimental data are essentially compatible with a first-order rate-controlling process. Similar results may be obtained by plotting log $[m_{Sr^{2+}}{}_s - m_{Sr^{2+}}{}_t]$. The systematic shift in the 50°C data may result from an erroneous estimate of the solubility at this temperature, from poor curve fitting, or most likely from a change of the rate-limiting mechanism at later stages. The 50°C data plot could be altered by slightly increasing the molalities of Sr^{2+} and HCO_3^- at equilibrium; nevertheless, the results shown in figure 7 constitute a good empirical fit of the experimental data with the first-order model.

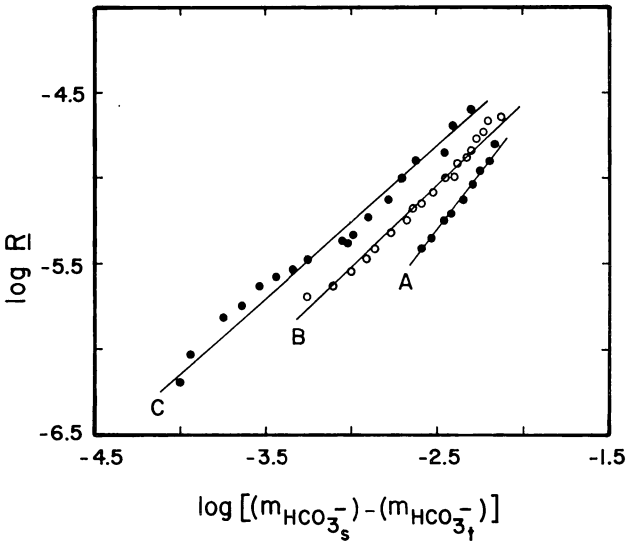

Fig. 6. This plot of log R versus log $[m_{HCO_3^-})_s - (m_{HCO_3^-})_t]$ demonstrates that the empirical rate law expressed by equation (20) is applicable. Lines A, B, and C representing data for 30°, 40°, and 50°C, have slopes of 1.30, 0.95, and 0.89 respectively.

Activation energies.—The effect of temperature upon the rate of strontianite dissolution was investigated under "free drift" conditions only. The expression of the change in reaction rate as a function of temperature commonly employs the use of the Arrhenius equation

$$\ln(k) = \ln(A) - (E_a/RT) \text{ or } k = Ae^{-(E_a/RT)} \qquad (22)$$

where k is the specific rate constant at the temperature of interest, T is the absolute temperature, R is the gas constant, A is the frequency (or preexponential) factor, and E_a is the apparent activation energy.

For first-order reactions the rate constant (expressed in sec^{-1}) may be determined either by the time-to-half-reaction method (Benson, 1960) or graphically from figure 7. The times to half saturation were 11,280, 7320, and 4080 sec for 30°, 40°, and 50°C, respectively. The corresponding rate constants are 6.14×10^{-5}, 9.47×10^{-5}, and 16.99×10^{-5} sec^{-1}. The activation energies from the 30° and 50°C data by the time-to-half-reaction method, from the slopes on figure 7 and from the slopes on a similar plot of log $(m_{Sr^{2+}s} - m_{Sr^{2+}t})$ versus time, are 9.9, 10.9, and 9.9 kcal, respectively. The value of 10 ± 2 kcal is believed to describe the activation energy for strontianite dissolution under the free drift experimental conditions.

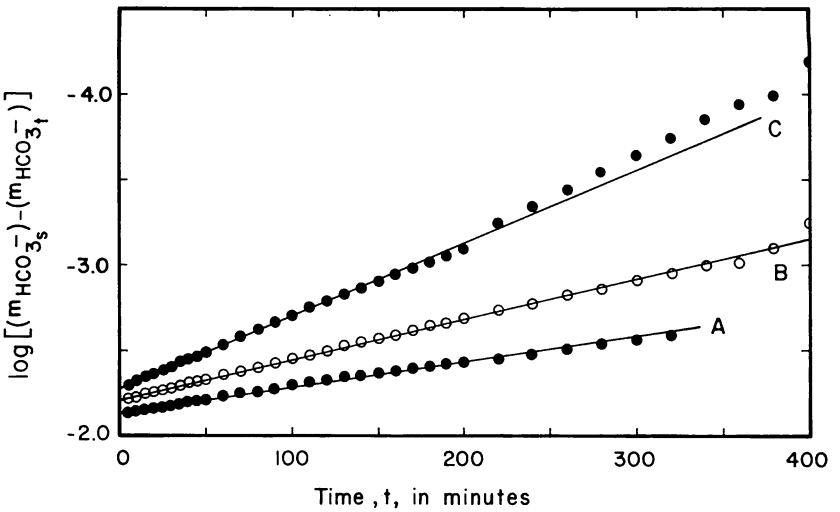

Fig. 7. Plot of log [($m_{HCO_3^-}$)$_s$ − ($m_{HCO_3^-}$)$_t$] versus time to test the applicability of the first-order hypothesis, equation (21), against the experimental data. Lines A, B, and C represent data for 30°, 40°, and 50°C respectively. Because dpH/dt is small in the later stages of the 50°C run, less weight was assigned to these points.

INTERPRETATION OF CONTROLLING PROCESSES

Controlling Process far from Equilibrium

Strontianite dissolution far from equilibrium was investigated at various constant pH values and at various partial pressures of carbon dioxide at a fixed pH. The first series of experiments resulted in data that described the effect of a dissociated acid on the dissolution rate. Under the experimental conditions the dissolution rate may be expressed as

$$R = k_1(a_{H^+})^{0.92} + k_2(a_{H^+})^{0.13} \tag{13}$$

The investigation of the effect of the partial pressures of carbon dioxide showed that the rate of reaction did not increase proportionally with the increase in associated acid (fig. 3) and that the data were compatible with the Langmuir adsorption isotherm (fig. 4). The assumption necessary to reach the second conclusion was that the corrected reaction rate, R' in equation (19), could be attributed to the change in the partial pressure of carbon dioxide. Combining the separate experiments results in a rate equation of the form

$$R = k_1(a_{H^+})^{0.92} + k_2(a_{H^+})^{0.13} + \frac{aP_{CO_2}}{1 + bP_{CO_2}} \tag{23}$$

This equation is experimentally valid at 40°C, at pH values ranging from 1.5 to 6.5 when $P_{CO_2} = 0$, and at pH = 4.5 when P_{CO_2} ranges from 0.0 to 0.78 atm.

The relative effectiveness of free acid, H^+, and associated acid, H_2CO_3, can be compared in terms of reaction rate constants from the experimental data. The rate of acid addition at pH = 4.5 under a nitrogen atmosphere was 0.109 ml/min and with $P_{CO_2} = 0.78$ atm was 0.869 ml/min. Assuming a first-order reaction for hydrogen ion catalysis yields

$$0.109 \text{ ml/min} = k_1(a_{H^+})$$

for which $k_1 = 10^{+3.54}$ ml/min. Subtracting the contribution for this reaction and assuming a first-order reaction for H_2CO_3 catalysis yields

$$0.760 \text{ ml/min} = k_2(a_{H_2CO_3})$$

for which $k_2 = 10^{+1.61}$ ml/min. Thus the ratio of k_1/k_2 is approximately 85 to 1 under these conditions.

The available data imply that for dissolution far from equilibrium, adsorption reactions with two aqueous species, H^+ and H_2CO_3, limit the dissolution rate and that the free hydrogen ion is about 85 times more effective than carbonic acid as a dissolution catalyst.

The observed kinetic phenomena may be interpreted as the reactions of a dissociated acid, H^+, and an associated acid, H_2CO_3, at the mineral surface. The mineral surface must have alternating zones of opposite charge because the lattice is not complete at the surface. For experiments run under a nitrogen atmosphere, it was assumed that all CO_2 is continuously removed from the system; thus all carbonate species have a fixed concentration gradient equal to their concentration at the mineral surface, as the bulk solution is assumed to be devoid of these species. If carbonate species were limiting the dissolution rate, there should be no significant difference in the dissolution rates at pH values of 1.5, 2.5, and 3.5. The large differences between the reaction rates at these low pH values (fig. 2) suggest that under these conditions the carbonate species resulting from strontianite dissolution do not significantly affect the dissolution rate. Therefore, the rate-limiting step is interpreted to be either the diffusion to or the interaction of a hydrogen ion at an anion position on the surface. It is postulated that the mineral surface is largely stripped of CO_3 species, leaving a surface relatively "enriched" with respect to strontium, and that diffusion of hydrogen ions to the underlying CO_3 sites or the formation of protonated CO_3 species at the underlying site (which weakens the bonding of the cation in the lattice) controls the dissolution rate in the low pH region. This interpretation is consistent with the point of zero charge model for carbonate minerals (Stumm and Morgan, 1970) and the experimental data and interpretation thereof for calcite (Somasundaran and Agar, 1967). The presence of very fine strontianite in the samples precluded the calculation of surface areas and diffusion coefficients; consequently, either diffusion or a chemisorption reaction may constitute the rate-limiting step under the experimental conditions. Similar studies upon calcite by Berner and Morse (1974) and

investigations by Plummer (personal commun., 1974) suggest that diffusion controls the dissolution rate of calcite under low pH conditions.

Controlling Process as Equilibrium is Approached

Various approaches using a_{H^+} were employed in analyzing the free-drift data. Previous investigators have had success in interpreting calcite dissolution kinetics by using the variable ΔpH (Berner and Morse, 1974). A slight variant of that method, plotting reaction rate against log $[(a_{H^+_t}) - (a_{H^+_s})]$, was also employed to test the experimental data. These two approaches, shown in figure 8, provided the best fit of the experimental data to equations relating the dissolution rate to hydrogen ion activities and molalities. The ΔpH plot shows an inflection at ΔpH = 0.35. The critical value is considerably larger than that determined for calcite by

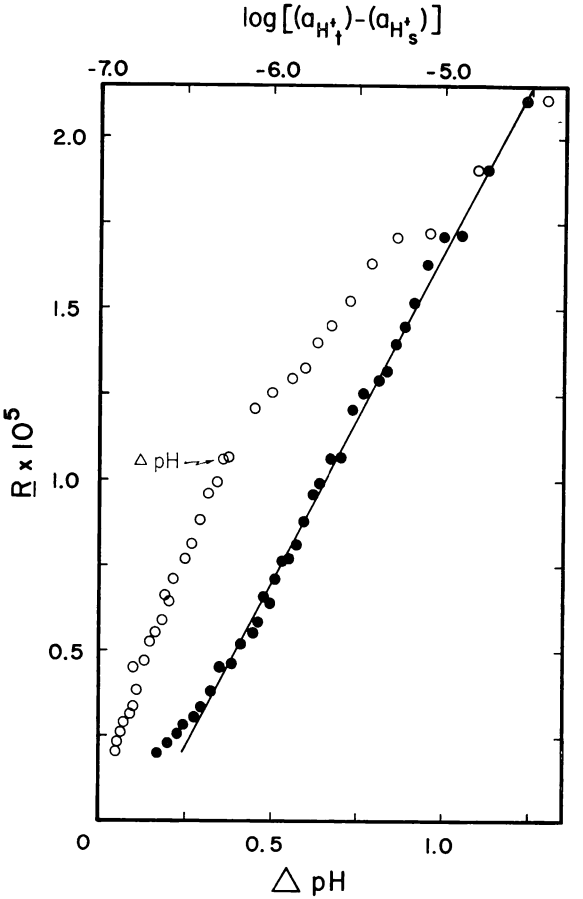

Fig. 8. Comparison of the variables ΔpH (open circles) and log $[(a_{H^+_t}) - (a_{H^+_s})]$ versus R for strontianite dissolution at 40°C and 0.78 atm P_{CO_2}.

Berner and Morse (1974). Also, the change in slope between the two regions is far less dramatic than that shown for calcite (compare fig. 1). The second plot in figure 8 differs from the first only in being the log of the difference of hydrogen ion activities, rather than the difference of the logs. Plotted in this manner, the data are very nearly linear until the reaction is closely approaching equilibrium (ΔpH <0.10). This late-stage shift may be due to an error in calculating the equilibrium pH (5.806, rounded to 5.81 earlier; note that extension of the late-stage ΔpH plot suggests that the equilibrium pH is 5.83). This type of plot is very sensitive to small errors when the difference in values considered approaches the confidence limit of the data, and the plot cannot be extrapolated to equilibrium [$\log (a_{H^+_t} - a_{H^+_s}) \rightarrow (-\infty)$].

An alternate approach to dissolution approaching equilibrium is depicted by figure 9, a plot of reaction rate versus [$(m_{HCO_3^-_s}) - (m_{HCO_3^-_t})$]. This figure shows that the mathematical expression for the first-order mechanism adequately describes the dissolution reaction as equilibrium is approached but fails in the early stages of the dissolution reaction. The early stage failure is not surprising when one considers that a maximum value (represented by the vertical line marked A) for the plotted variable exists at the start of an experiment, and that in the initial stages significant pH changes cause only small changes in the plotted variable. As the pH value approaches the pK_1 value, however, ($pK_1 - pH \leq 0.5$) the first-order bicarbonate mechanism becomes compatible with the experimental data.

These data could possibly be interpreted to signify that a critical level of HCO_3^- must exist in the bulk solution before the back reaction (that is, local reprecipitation of $SrCO_3$) becomes effective, but such a suggestion would be highly speculative if based solely upon the data from this study. In addition, the logarithmic parameter [$\log (a_{H^+_t} - a_{H^+_s})$], although providing an excellent mathematical fit of the data, does not lend itself to a reasonably simple interpretation of the dissolution mechanism.

The linearity of the data and the slope of approximately one shown in figure 9 indicate that the dissolution of strontianite can be more simply interpreted in terms of reactant adsorption for the precipitation reaction or product removal for the dissolution reaction at the mineral surface. Only one reaction mechanism is required to explain the kinetic behavior over most or all the experimental range.

A first-order relationship between R and ($m_{Sr^{2+}_s} - m_{Sr^{2+}_t}$) should also be valid, because, for the experiments that approach equilibrium, the dissolution reaction is basically

$$SrCO_{3(s)} + H_2CO_3 = Sr^{2+} + 2HCO_3^-$$

and electrical neutrality is maintained by increasing HCO_3^- concentrations. Plots similar to figures 6, 7, and 9 show that there is essentially no

difference in the quality of fit for a first-order reaction controlled by $[(m_{HCO_3^-})_s - (m_{HCO_3^-})_t]$ or $[(m_{Sr^{2+}})_s - (m_{Sr^{2+}})_t]$. The dependence upon $m_{HCO_3^-}$ might be interpreted as either an adsorption of an associated acid at the mineral surface or, combined with $m_{Sr^{2+}}$ dependence, as a precipitation (that is, back) reaction at the mineral surface.

To test these mechanisms for precipitation control of the overall rate, certain preliminary assumptions were made. They are that the concentration of carbonic acid, H_2CO_3, is maintained by the fixed partial pressure of carbon dioxide, is constant throughout the experimental runs, and does not cause changes in the reaction rate during these runs. Aqueous diffusion is believed not to be the rate-limiting step for the dissolution of strontianite, because of the similar reaction rates under stirred and un-

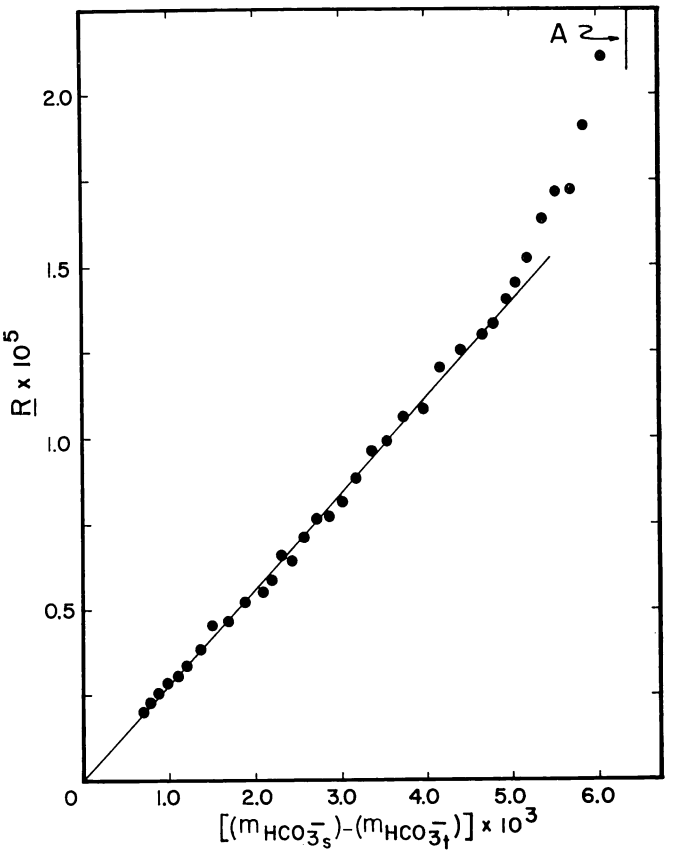

Fig. 9. Plot of $[(m_{HCO_3^-})_s - (m_{HCO_3^-})_t]$ versus R for strontianite dissolution at 40°C and 0.78 atm P_{CO_2}. The symbol A designates the limiting value (initial condition at t = 0) for the variable $[(m_{HCO_3^-})_s - (m_{HCO_3^-})_t]$.

stirred conditions and because the activation energy is considerably higher than the 4.5 kcal per mole expected for aqueous diffusion.

The fact that n is approximately equal to 1 suggests that a back reaction is affecting the overall reaction rate. The hypothesis employed is that the mechanism for this surface reaction is the same for dissolution as for precipitation (principle of microscopic reversibility). There is no experimental proof to support this hypothesis, but it is the simplest possible assumption, and in the absence of negative evidence it is preferred to a more complicated one.

The overall reaction rate, which is experimentally determined, may be expressed as

$$R = R_f - R_b \tag{24}$$

where R is the overall reaction rate, R_f is the forward reaction rate, R_b is the back reaction rate. Two approaches using the rate information determined far from equilibrium were employed to determine the forward reaction rate in order to calculate the back reaction rate.

One method of calculating the forward reaction rate is to use the data obtained far from equilibrium assuming that the back reaction is not yet significant. Combining the first and third terms of equation (23) into one constant, the predicted forward rate is

$$R_f = 3.08 \times 10^{-5} + 8.65 \times 10^{-6} (a_{H^+})^{0.13} \tag{25}$$

A second option is to assume that the forward reaction rate is constant, which means that the forward rate is zero-order reaction. This would be the case if the adsorption of H_2CO_3 at the mineral surface were the rate-limiting step for the forward reaction. The back reaction rate was calculated by subtracting the observed rate from the calculated forward reaction rate. Both methods of calculating the forward reaction rate yield a nonlinear plot for the first 25 min of the reaction; however, the calculated back reaction rates using equation (25), listed in table 4, provide a better data fit of the variables tested for the period from 30 to 400 min; figure 10, a plot of R_b versus $[(m_{HCO_3^-})_s - (m_{HCO_3^-})_t]$, represents the best data fit of the investigated variables. The intercept value, or rate at equilibrium, is slightly lower (7 percent) than predicted from the experimental values determined far from equilibrium (pH = 4.5). The maximum value that $[(m_{HCO_3^-})_s - (m_{HCO_3^-})_t]$ can attain is the value at t = 0 and is shown by the symbol A. A better fit of the data obtained while approaching equilibrium might be possible if the constant and the exponent in equation (25) were adjusted, but this would negate the value of the rate experiments performed far from equilibrium. Plotting R_b versus $m_{HCO_3^-}$, determined that substituting $m_{HCO_3^-}$ for $[(m_{HCO_3^-})_s - (m_{HCO_3^-})_t]$ did not improve the quality of the data fit.

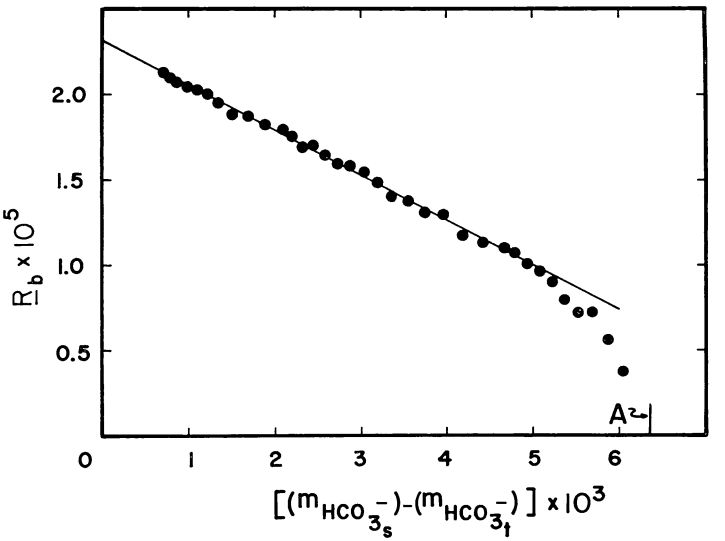

Fig. 10. Plot of $[(m_{HCO_3^-})_s - (m_{HCO_3^-})_t]$ versus R_b, the back reaction rate calculated using equation (25). The data are for strontianite dissolution at 40°C and 0.78 atm P_{CO_2}.

Because the forward reaction rate for the free drift experiments at pH conditions greater than 4.5 seems to be controlled by a surface reaction (tentatively believed to be proton adsorption at the mineral surface), it is logical to conclude that the correspondence between the calculated back reaction rate and $m_{HCO_3^-}$ represents a deprotonation reaction.

SUMMARY

This study was undertaken to investigate the dissolution kinetics of strontium carbonate. The major conclusions are:

1. Strontianite dissolution, far from equilibrium for pH values ranging from 1.5 to 6.5 and with a continuously renewed N_2 gas phase, may be expressed by the equation:

$$dm_{Sr^{2+}}/dt = k_1(a_{H^+})^{0.92} + k_2(a_{H^+})^{0.13} \text{ mole} \cdot \text{min}^{-1}$$

where $k^1 = 2.4 \times 10^3\ k_2$. The rate-limiting step is believed to be protonation of the lattice anion or diffusion of H^+ to the CO_3^{2-} lattice anion.

2. Strontianite dissolution, far from equilibrium at a pH of 4.5 and with a continuously renewed N_2–CO_2 gas phase, may be expressed by the following equation employing the Langmuir adsorption isotherm

$$dm_{Sr^{2+}}/dt = k_3 + \frac{aP_{CO_2}}{1 + bP_{CO_2}}$$

where $k_3 = 2.35 \times 10^{-6}$ mole•min^{-1}, $a = 1.54 \times 10^{-4}$ mole•min^{-1}•atm^{-1}, and $b = 5.05$ mole•min^{-1}•atm^{-1}. The investigation showed that increasing the concentration of the reaction product, H_2CO_3, increased the dissolution rate. This indicates that carbonic acid or one of its ionization products, HCO_3^- and CO_3^{2-}, facilitates the dissolution process. If deprotonation of carbonic acid at the mineral surface (that is, proton transfer from H_2CO_3 to the lattice anion) is the mechanism that facilitates dissolution, then the effectiveness of carbonic acid is approximately 0.012 times that of the hydronium ion.

3. Strontianite dissolution as equilibrium is approached seems to be controlled by a surface reaction for the conditions investigated. The dissolution rates were not affected by different stirring conditions, and the calculated activation energy, 10 ± 2 kcal, is con-

TABLE 4

Calculated forward and back reaction rates

Time in min	pH	Calculated $R_f \times 10^5$ (eq 25)	Observed $R \times 10^5$	Calculated $R_b \times 10^5$ (eq 24)
5	4.513	2.493	2.113	0.380
10	4.714	2.467	1.906	0.561
15	4.842	2.450	1.721	0.729
20	4.941	2.438	1.716	0.722
25	5.018	2.428	1.633	0.795
30	5.079	2.419	1.518	0.901
35	5.130	2.413	1.447	0.966
40	5.174	2.407	1.396	1.011
45	5.212	2.403	1.323	1.080
50	5.246	2.398	1.294	1.104
60	5.305	2.390	1.255	1.135
70	5.355	2.384	1.211	1.173
80	5.395	2.378	1.079	1.299
90	5.431	2.374	1.063	1.311
100	5.462	2.370	0.992	1.378
110	5.490	2.366	0.962	1.404
120	5.514	2.363	0.878	1.485
130	5.535	2.360	0.811	1.549
140	5.554	2.358	0.770	1.588
150	5.572	2.355	0.763	1.592
160	5.588	2.353	0.707	1.646
170	5.602	2.352	0.642	1.710
180	5.616	2.350	0.664	1.686
190	5.628	2.348	0.587	1.761
200	5.639	2.346	0.553	1.793
220	5.659	2.344	0.523	1.821
240	5.676	2.342	0.465	1.877
260	5.692	2.340	0.455	1.885
280	5.705	2.339	0.383	1.956
300	5.716	2.337	0.324	2.013
320	5.726	2.335	0.311	2.024
340	5.735	2.334	0.297	2.047
360	5.743	2.333	0.260	2.073
380	5.750	2.332	0.232	2.100
400	5.756	2.332	0.202	2.130

siderably greater than would be expected for an aqueous-diffusion rate-controlling mechanism.

4. The back reaction rate for strontianite dissolution is believed to be controlled by adsorption and deprotonation of HCO_3^- at the mineral surface. The back reaction rate for strontianite dissolution approaching equilibrium was calculated using the dissolution rates obtained far from equilibrium. Both first-order variables, $[(m_{HCO_3^-})_s - (m_{HCO_3^-})_t]$ and $[(m_{Sr^{2+}})_s - (m_{Sr^{2+}})_t]$, provided satisfactory agreement with the calculated back reaction rate, but the principle of microscopic reversibility suggests that Sr^{2+} is not the rate-limiting species for the back reaction.
5. The solubility products for strontianite at 25°, 30°, 40°, and 50°C were determined to be $10^{-9.235}$, $10^{-9.27}$, $10^{-9.33}$, and $10^{-9.40}$, respectively.

ACKNOWLEDGMENTS

Support for the laboratory investigation was provided by the Geoscience Department, New Mexico Institute of Mining and Technology, through a research assistantship. Computer facilities to reevaluate the experimental data neglecting ion pairs (Jacobson and Langmuir, 1974) were provided by the Georgia District, United States Geological Survey, Water Resources Division, thanks to H. E. Gill. Terry Kramer and Roger Holmes aided in drafting the figures. Publication costs were paid by the Montana Bureau of Mines and Geology, a division of the Montana College of Mineral Science and Technology.

Critical review and suggestions by Neil Plummer and John Morse are appreciated by the authors. Dr. Plummer's detailed questions and suggestions considerably improved the clarity of the final manuscript.

REFERENCES

Benson, S. W., 1960, The foundations of chemical kinetics: New York, McGraw-Hill, 703 p.

Berner, R. A., and Morse, J. W., 1974, Dissolution kinetics of calcium carbonate in sea water. IV. Theory of calcite dissolution: Am. Jour. Sci., v. 274, p. 108-134.

Berner, R. A., and Wilde, Pat, 1972, Dissolution kinetics of calcium carbonate in sea water. I. Saturation state parameters for kinetic calculations: Am. Jour. Sci., v. 272, p. 826-839.

Campbell, J. R., and Nancollas, G. H., 1969, The crystallization and dissolution of strontium sulfate in aqueous solution: Jour. Phys. Chemistry, v. 73, p. 1735-1740.

Carpenter, A. B., and Miller, J. C., 1969, Geochemistry of saline subsurface water, Saline County (Missouri): Chem. Geology, v. 4, p. 135-167.

Curl, R. L., 1968, Solution kinetics of calcite: Internat. Cong. Speleology, 4th, Yugoslavia 1965, Proc., v. 3, p. 61-66.

Denbigh, K., 1966, The principles of chemical equilibrium: Cambridge, Cambridge Univ. Press, 494 p.

Gaines, A. M., and Heffner, J. D., 1973, Dolomitization: A new experimental approach [abs.]: Geol. Soc. America Abs. with Program, v. 5, no. 7, p. 628.

Gardiner, W. C., Jr., 1969, Rates and mechanisms of chemical reactions: New York, W. A. Benjamin, 284 p.

Garrels, R. M., and Christ, C. W., 1965, Solutions, minerals and equilibria: New York, Harper and Row, 450 p.

Garrels, R. M., Thompson, M. E., and Siever, R., 1960, Stability of some carbonates at 25°C and one atmosphere total pressure: Am. Jour. Sci., v. 258, p. 402-418.

Helgeson, H. C., 1967, Solution chemistry and metamorphism, *in* Ableson, P. H., ed., Researches in geochemistry, v. 2: New York, John Wiley & Sons, p. 362-404.

Jacobson, R. L., and Langmuir, Donald, 1974, Dissociation constants of calcite and $CaHCO_3^+$ from 0 to 50°C: Geochim. et Cosmochim. Acta, v. 38, p. 301-318.

Kern, D. M., 1960, The hydration of carbon dioxide: Jour. Chem. Ed., v. 37, no. 1, p. 14-23.

Levenspiel, O., 1972, Chemical reaction engineering, 2d ed.: New York, John Wiley & Sons, 578 p.

Liu, S., and Nancollas, G. H., 1971, The kinetics of dissolution of calcium sulfate dihydrate: Jour. Inorg. Nuclear Chemistry, v. 33, p. 2311-2316.

Maron, S. H., and Prutton, C. F., 1958, Principles of physical chemistry, 3d ed.: New York, MacMillan, 789 p.

Mitterer, R. M., and Carter, P. W., 1973, Some analytical and experimental results bearing on the precipitation of $CaCO_3$ [abs.]: Geol. Soc. America Abs. with Program, v. 5, no. 7, p. 741.

Morse, J. W., 1974a, Dissolution kinetics of calcium carbonate in sea water. III. A new method for study of carbonate reaction kinetics: Am. Jour. Sci., v. 274, p. 97-107.

———— 1974b, Dissolution kinetics of calcium carbonate in sea water. V. Effects of natural inhibitors and the position of the chemical lysocline: Am. Jour. Sci., v. 274, p. 638-647.

Plummer, L. N., and Mackenzie, F. T., 1974, Predicting mineral solubility from rate data: Application to the dissolution of magnesian calcites: Am. Jour. Sci., v. 274, p. 61-83.

Prigogine, I., Outer, P., and Herbo, C., 1948, Affinity and reaction rate close to equilibrium: Jour. Phys. Chemistry, v. 52, p. 321-331.

Somasundaran, P., and Agar, G. E., 1967, The zero point of charge of calcite: Jour. Colloid and Interface Sci., v. 24, p. 433-440.

Stumm, W., and Morgan, J. J., 1970, Aquatic chemistry: New York, Wiley Intersci., 583 p.

Walls, R. A., 1973, Dissolution kinetics of incompatible strontium and magnesium in carbonate skeletal material [abs.]: Geol. Soc. America Abs. with Program, v. 5, no. 7, p. 854.